ORIGINAL ARTICLE

Phenotypic characterization of C57BL/6J mice carrying the *Disc1* gene from the 129S6/SvEv strain

Liang-Wen Juan · Chun-Chieh Liao · Wen-Sung Lai · Chia-Yuan Chang · Ju-Chun Pei · Wan-Rong Wong · Chih-Min Liu · Hai-Gwo Hwu · Li-Jen Lee

Abstract Disruption of disrupted-in-schizophrenia 1 (DISC1), a candidate susceptibility gene for schizophrenia, was first identified in a large Scottish family in which many members suffered from various psychiatric disorders, including schizophrenia. To model the Scottish DISC1 truncation, we established a *Disc1* mutant mouse line in which the 129S6/SvEv 25-bp deletion variant was transferred into the C57BL/6J strain by backcrossing. A battery of behavioral tasks was conducted to evaluate the basic behaviors and cognitive function of these mice. In heterozygote and homozygote *Disc1* mutant (Het and Homo) mice, behavioral impairments were noted in working memory test which is thought to be mediated by the function of the medial prefrontal cortex (mPFC). The properties of mPFC neurons were characterized in both morphological and physiological aspects. The dendritic diameters were decreased in layer II/III mPFC pyramidal neurons of Het and Homo mice, whereas a significant reduction in spine density was observed in Homo mice. Neuronal excitability was declined in layer II/III mPFC pyramidal neurons of Het and Homo mice, yet increased transmitter release was identified in Homo mice. Thus, the structural and functional alterations of the mPFC in Het and Homo mice might account for their cognitive impairment. Since most of the gene knockout mice are generated from 129 substrain-derived embryonic stem cells, potential *Disc1* deficiency should be considered.

Keywords Schizophrenia · Working memory · Medial prefrontal cortex, dendrite · Dendritic spines · Neuronal excitability · Synaptic transmission

L.-W. Juan and C.-C. Liao contributed equally to this work.

L.-W. Juan · C.-C. Liao · L.-J. Lee (✉)
Graduate Institute of Anatomy and Cell Biology,
College of Medicine, National Taiwan University,
No. 1, Ren-Ai Rd, Section 1, Taipei 100, Taiwan, ROC
e-mail: ljlee@ntu.edu.tw

W.-S. Lai · C.-Y. Chang · J.-C. Pei
Department of Psychology, Taiwan University Hospital,
Taipei, Taiwan, ROC

W.-S. Lai · W.-R. Wong · C.-M. Liu · H.-G. Hwu · L.-J. Lee
Graduate Institute of Brain and Mind Sciences,
Taiwan University Hospital, Taipei, Taiwan, ROC

W.-S. Lai · C.-M. Liu · H.-G. Hwu · L.-J. Lee
Neurobiology and Cognitive Sciences Center,
National Taiwan University, Taipei, Taiwan, ROC

C.-M. Liu · H.-G. Hwu
Department of Psychiatry, National Taiwan University Hospital,
Taipei, Taiwan, ROC

Introduction

Schizophrenia is a severe mental disorder that affects approximately 1 % of the world's population. Accumulating data suggest that dysregulation of molecules associated with the development of neural circuits might contribute to the pathogenesis of schizophrenia (Mei and Xiong 2008; Jaaro-Peled et al. 2009; Brandon and Sawa 2011; Penzes et al. 2011; Arguello and Gogos 2012).

One of the candidate susceptibility genes for schizophrenia that play important roles in neural development is disrupted-in-schizophrenia 1 (DISC1) (Mackie et al. 2007; Brandon and Sawa 2011) which was originally discovered as a putative gene for major psychiatric disorders in a Scottish pedigree (Millar et al. 2000). DISC1 proteins are highly expressed in the developing brain (Schurov et al. 2004) and the roles of DISC1 in neuronal proliferation,

migration, regulation of spines and synapses have been demonstrated in various experimental models (Kamiya et al. 2005; Mao et al. 2009; Hayashi-Takagi et al. 2010; Ishizuka et al. 2011; Wang et al. 2011; Steinecke et al. 2012).

The breakpoint of DISC1 in the Scottish family is immediately after exon 8 (Millar et al. 2000). To model Scottish DISC1 gene disruption in mice, different engineering strategies were used, and diverse phenotypes have been reported (Koike et al. 2006; Hikida et al. 2007; Li et al. 2007; Kvajo et al. 2008, 2011; Pletnikov et al. 2008; Shen et al. 2008; Ayhan et al. 2011). Transgenic mice that possess two copies of the truncated Disc1 gene encoding the first eight exons exhibit abnormalities in brain structure, dendritic profiles and attention/emotion-related behaviors (Shen et al. 2008). Mice that express αCaMKII-driven dominant-negative C-terminal truncated human DISC1 have impaired sensorimotor gating, sociability and dendritic complexity (Hikida et al. 2007; Pletnikov et al. 2008). To generate a truncated DISC1 transcript and protein, a sequence including an artificial stop codon plus a polyadenylation tail was knocked in at the end of exon 8 of mouse Disc1 gene, resulting in a knock-in, $Disc1^{Tm1Kara}$ strain (Koike et al. 2006). After backcrossing to C57BL/6J background (>5 generations), the 100-kDa full-length Disc1 protein is abolished, and impaired working memory, dendritic architecture, and synaptic properties are evident in $Disc1^{Tm1Kara}$ mice (Koike et al. 2006; Kvajo et al. 2008, 2011). However, $Disc1^{Tm1Kara}$ line was generated using mouse embryonic stem cells from a 129S6/SvEv background. In this strain, there is a 25-bp deletion in exon 6 of the Disc1 gene, which induces a shift of the reading frame and a premature stop codon in exon 7 (Koike et al. 2006).

Here, we report a Disc1 mutant mouse line in which the 129S6/SvEv 25-bp deletion variant has been transferred into the C57BL/6J strain by more than ten generations of backcrossing. Behavioral, anatomical and physiological phenotypes of these mice were characterized. Our findings indicate structural and functional deficits in the medial prefrontal cortex (mPFC) in both homozygous and heterozygous Disc1 mutant mice.

Materials and methods

Animals

All animals were bred and housed in the Laboratory Animal Center College of Medicine, National Taiwan University, under a 12-h light/dark (0800/2000 hours) cycle with free access to food and water. All animal experiments were performed in accordance with the guidelines set by the Institutional Animal Care and Use Committee of the College of Medicine, National Taiwan University. Adult (over 8 weeks old) male wild-type (WT), heterozygote Disc1 mutant (Het) and homozygote Disc1 mutant (Homo) mice were used in this study. Subsequent to behavioral examinations, mice were used histological and electrophysiological examinations.

Generation and genotyping of Disc1 mutant mice

Disc1 mutant mice were generated by introducing the 25-bp deletion variant in exon 6 and the premature termination codon at exon 7 of 129S6/SvEv mice into C57BL/6J mice by backcrossing over ten generations at Level Biotechnology Inc., Taipei, Taiwan. The presence of the 25-bp deletion in exon 6 of the 129S6/SvEv mDISC1 transcript in genomic DNA isolated from tails of each backcross generation was confirmed by PCR genotyping using a primer set (forward 5′-GCTGTGACCTGATGGCAC-3′; reverse 5′-GCAAAGTCACCTCA ATAACCA-3′) flanking exon 6.

For cDNA sequencing, brain tissues from WT and Homo mice were collected. RNA was extracted and reverse transcribed into cDNA using the SuperScript® III first-strand synthesis system (Invitrogen, Carlsbad, CA, USA), amplified by PCR using a primer set (forward primer: 5′-ACGGATGTCTGCGCTGGAGG-3′, reverse primer: 5′-TCTGACAGCCAGGTT CAGTG-3′) and purified using a Gel/PCR DNA fragment extraction kit (Geneaid, Taipei, Taiwan, ROC). Finally, the products were sequenced using a DNA Analyzer (Applied Biosystems, Foster City, CA, USA).

To check the expression of Disc1 protein, western blot analysis was performed. In brief, the brains of P8 mice were quickly dissected, frozen in liquid nitrogen, and stored at −80 °C until protein extraction. Tissue samples were homogenized in lysis buffer [25 mM Tris (pH 8.0), 125 mM NaCl, 1 % Triton and Inhibitor Cocktails] (Sigma, St. Louis, MO, USA), and then centrifuged at 14,000 rpm at 4 °C for 20 min. The same amount of protein was separated by 10 % SDS-PAGE in running buffer (192 mM glycine, 25 mM Tris-base, 0.1 % SDS) and transferred onto a nitrocellulose membrane (Millipore, Billerica, MA, USA). The membrane was blocked using 5 % skim milk in TBS with 0.1 % Tween 20 (TBS-T) for 1 h with gentle agitation. The membrane was then incubated in rabbit anti-DISC1-N-terminal polyclonal antibody (1:100, kindly provided by Dr. Joseph Gogos) and rabbit anti-GAPDH monoclonal antibody (1:1,000, Cell Signaling, Danvers, MA, USA) overnight at 4 °C, with gentle agitation. The membrane was incubated in horseradish peroxidase-conjugated goat anti-rabbit IgG secondary antibody (Vector labs, Burlingame, CA, USA) for 1 h. Bound antibody was detected using an ECL chemiluminescence kit (Millipore) on super RX film (Fujifilm, Tokyo,

Japan), and densitometric analysis was performed using ImageJ software (NIH, Bethesda, MD, USA).

Behavioral phenotyping of *Disc1* mutant mice

Adult WT, Het and Homo male mice were subjected to behavioral tests, which were conducted between 1000 and 1600 hours. A battery of behavioral tasks was conducted to evaluate the basic behaviors and cognitive functions in two batches of mice. The sequence of the tests was fixed. The minimal interval between behavioral tests was 1 day. Before tests began, mice were taken to the experimental environment for habituation for at least 30 min.

Elevated plus maze test

The elevated plus maze was used to evaluate anxiety-related behaviors. The custom-made maze consists of two white plastic open arms (40 × 6 cm), crossed at a right angle by two arms of the same dimensions, enclosed by 20-cm high walls of the same material as the closed arms. The maze is located 50 cm above the floor. Mice were tested by placing them on the central platform of the maze, facing one of the open arms, and letting them to move freely for 10 min. The behaviors were continuously videotaped with a video camera placed above the apparatus and then analyzed with Topscan software (Clever System, Reston, VA, USA). The travelled distance and the time spent in the open arms, closed arms and central region were quantified.

Forced swimming test

The forced swimming test was used to estimate depression-like behaviors. Individual mice were confined in narrow Plexiglas cylinders (25 cm height, 10 cm internal diameter) filled with water (25 °C, 15 cm height). Three behavioral parameters, including struggling (animal reached its forepaws out of the water, demonstrating the motivation to escape), immobility (animal stayed in the water without struggling, except keeping its head above the water and balancing for more than 2 s) and swimming (animal tried to keep its body from sinking by moving its hind paws) were characterized. The time spent in each behavior was measured during the last 6 min of the 8-min test period.

Novel object recognition test

This test was used to assess memory for interactions with a novel object. During the habituation phase, a mouse was placed in an open field (40 cm × 40 cm) for 10 min twice a day for 2 days before the test. In the test phase, the mouse was placed in the open field, presented with a pair of identical objects and allowed to freely explore for 8 min. After exploration, the mouse was removed and placed back in the open field 10 min later. This time, one of the original objects was replaced by a novel one, and the animal was allowed to explore the objects freely for 8 min. The time of exploration of the objects (including any investigative behavior, such as deliberate contact or touching with the nose) was quantified. To reduce odor cues, the open field apparatus and the objects were thoroughly cleaned with 10 % alcohol, dried and ventilated for a few minutes between mice.

Y-maze

The Y-maze was used to quickly estimate the spatial memory of these mice. The Y-maze consists of three equal-sized arms (30 × 10 cm) interconnected at 120°. A mouse was first placed in one arm (start arm) of the maze with one arm blocked. The unblocked arm other than the start arm was defined as the "familiar arm." The mouse was allowed to freely explore in the start and familiar arms for 10 min. After exploration, the mouse was removed and placed back to the maze 1 h later. This time, the originally blocked arm was opened and defined as the "novel arm," and the mouse was allowed to freely explore for 10 min. The activities were continuously recorded by a video camera placed above the maze. The distance travelled and time spent in the three arms and central region were quantified by Topscan software (Clever System).

Morris water maze

The spatial learning and memory abilities in mice were evaluated by the Morris water maze test. Briefly, a pool (100 cm in diameter) was divided into four quadrants and filled with milky water. A platform (12 cm in diameter) was placed at the center of a fixed quadrant, 2 cm below the water surface. A mouse was released from one of the four start points with the head facing the wall into the pool and allowed to freely search for the hidden platform using three visual cues. If the mouse was not able to locate the platform in 2 min, a gentle guide was provided. Each mouse was allowed to stay on the platform for 30 s. After a 1-min interval, the mouse was released into the pool from another start point. Four trials were administered per day for five consecutive days. The 5-day period was defined as the training phase. For all of the trials, the latency and swimming path from release to reaching the platform was recorded. Retention (memory) was assessed with a probe trial given 1 h after the last training trial in the fifth training day. In the probe trial, the hidden platform was removed, and the swim path and time of each mouse were recorded with a video camera and subsequently analyzed by Topscan software.

Delayed non-match to place task

The working memory of mice was evaluated using a delayed non-match to place task, which is considered to be an mPFC-related task. Prior to the experiment, mice were food-restricted to 85–90 % of their original weight. The body weight was maintained through the test period. Small pieces of food pellets were placed at two ends of the T-maze as a reward. After 2 days of habituation to the T-maze (10 min/day), 2 days of forced alternation in the T-maze with the blocked opposite arm were conducted. In the training phase, a mouse was placed in the T-maze, forced turn to one arm, and the food reward at the terminal was consumed. After a 5-s delay, the mouse was placed in the T-maze again; to receive the food reward, the mouse was required to turn to the opposite side. When a mouse exhibited an accuracy rate >80 % for three consecutive days, the testing phase was started. If not, the training phase was prolonged until the mouse fulfilled the required criteria. The number of days required to learn the criteria and the accuracy were recorded. In the testing phase, the delayed time was set to be 5, 15, 30, 45, and 60 s. The accuracy in each delay condition was calculated.

Histology

Adult WT, Het and Homo male mice were deeply anesthetized by intraperitoneal injection of 2.5 % Avertin and perfused transcardially with normal saline followed by 4 % paraformaldehyde in 0.1 M phosphate buffer (PB, pH 7.4). Whole brains were taken and postfixed overnight in the same fixative at 4 °C.

Examination of overall brain structure

The overall brain structure including thickness of the cerebral cortex, corpus callosum and the volume of the lateral ventricles was measured. Coronal sections of brain samples of 50 μm thickness were cut using a vibratome and imaged. The thickness of cortex was measured from the surface to the white matter of the cortex at the point tangent to the surface by a imaginary line 45° deviated from the midline. According to the mouse brain atlas (Franklin and Paxinos 2008), the cortical regions we measured are likely to be the somatosensory cortex. The thickness of corpus callosum was measured at the midline of the section. The volume of lateral ventricle was estimated as the area multiplied the thickness and number of sections.

Golgi stain

To reveal the morphological features of dendrites, the Golgi–Cox method was used. Brain samples were collected and placed in impregnation solution from the FD Rapid GolgiStain kit (NeuroTechnologies, Ellicott City, MD, USA) at room temperature for 3 weeks. Impregnated samples containing the mPFC were transferred into H_2O for 2 days and then cut at a thickness of 150 μm using a vibratome. Sections were incubated with a mixture of developer and fixer solutions (FD Rapid GolgiStain kit), washed, mounted, and examined under a light microscope (Olympus, Tokyo, Japan) with a 40× lens for dendritic morphology and a 100× oil lens for spine analysis. Stacks of images were constructed using the StereoInvestigator system (Microbrightfield Bioscience, Williston, VT, USA).

Layer II/III pyramidal neurons in the mPFC without obvious truncation in their dendritic profiles were selected for morphometric examination. The morphology of selected neurons was reconstructed and analyzed with Neurolucida software (Microbrightfield Bioscience). Sholl and branched structure analyses in the Neurolucida Explorer software toolbox were used to quantify the topological parameters (e.g., number of primary dendrites, branching nodes, dendritic segments, and terminal endings) and size-related parameters (e.g., dendritic length and intersections and terminal endings at different distances from the soma). The lengths of dendritic segments that were classified as intermodal (between 2 bifurcation nodes) or terminal (between the bifurcation node and terminal ending) were measured into different orders. The density of the dendritic spines was also determined and expressed as the number of spines per μm of the dendrite's length.

Electrophysiology

Acute mPFC brain slices of 300-μm thickness were prepared from adult mice. Slices were maintained and recorded at 32–34 °C in artificial CSF (ACSF; compositions in mM: 1.8 $MgSO_4$, 124 NaCl, 3 KCl, 1.3 $NaH_2PO_4 \cdot 2H_2O$, 1.6 $CaCl_2$, 26 $NaHCO_3$, 20 glucose) saturated with 95 % O_2 and 5 % CO_2. Whole-cell patch-clamp recordings were performed on layer II/III pyramidal neurons in the mPFC using a Multiclamp 700B amplifier (Molecular Devices, Sunnyvale, CA, USA). The patch electrodes were pulled from filamented borosilicate glass (Harvard apparatus, Holliston, MA, USA) by a P-87 puller (Sutter instruments, Novato, CA, USA) and filled with a potassium-based internal solution containing (in mM): 117 K-gluconate, 13 KCl, 1 $CaCl_2$, 2 $MgCl_2$, 11 EGTA, 10 HEPES, 2 Na_2-ATP and 0.5 Na-GTP (pH 7.4, 306 mOsm). Data were collected (10 kHz sampling rate) using pClamp 10.1 (Molecular Devices) and analyzed with Clampfit. To monitor the health of the cell, input and series resistances were continuously monitored, and only data from cells in which these parameters remained stable throughout the recording were used for further analysis.

In current-clamped whole-cell recordings, we measured the resting membrane potential (V_m) and input resistance (R_{in}). The membrane time constant (τ) was determined by fitting the change of membrane potential from the resting potential to −80 or −90 mV with a single exponential function. A series of current injection steps (range −200 to +500 pA with 20 pA per step) were given to evoke action potentials (APs). Single-AP properties, including threshold, amplitude, and amplitude of the afterhyperpolarization (AHP), were measured from the first induced AP. The parameters of AP were determined as previously described (Liao and Lee 2011).

In voltage-clamped whole-cell recordings, spontaneous excitatory postsynaptic currents (sEPSCs) and evoked PSCs (ePSCs) were recorded in the presence of 10 μM gabazine, a GABA$_A$ receptor blocker, at −70 mV. Electrical stimulation was applied through an electrode consisting of tungsten wire. The stimulating electrode was placed near layer I, 1 mm dorsal to the location of whole-cell recordings in layers II/III. The frequency and amplitude of sEPSCs and ePSCs were averaged and analyzed.

Data analysis

Behavioral data were analyzed with repeated measures or one-way ANOVA with genotype as the factor. Two-tailed unpaired Student's t test was applied to analyze the morphometric and electrophysiological data. Data were expressed as the mean ± SEM. Significant level was set as $p < 0.05$.

Results

Generation and verification of Disc1 mutant mice

The *Disc1* gene is truncated in 129S6/SvEv and in other 129 substrains (Koike et al. 2006; Clapcote and Roder 2006). In this study, *Disc1* mutant mice were generated by crossing 129S6/SvEv mice with C57BL/6J mice for more than ten generations. As depicted in Fig. 1a, the 25-bp deletion in exon 6 of the 129S6/SvEv *Disc1* allele (Disc1 mutant) results in a premature stop codon of *Disc1* in exon 7 (*, TGA). The 129S6/SvEv *Disc1* allele was transferred to C57BL/6J strain and confirmed by cDNA sequencing (Fig. 1b). Homozygous *Disc1* mutant (Homo) mice carried only the 25-bp deleted allele, whereas heterozygous *Disc1* mutant (Het) mice carried both wild-type (WT) and 25-bp deleted alleles (Fig. 1c). To check the expression of Disc1 protein, western blot analysis using specific antibody (kindly provided by Dr. Joseph Gogos) was performed. Unlike in WT, a 100-kDa Disc1 isoform was absent in Homo mice and significantly reduced in Het mice. A

70 kDa band was not detected in Homo and largely reduced in Het mice (Fig. 1d). However, many bends were still present in all three genotypes, representing either non-specific cross reaction of the antibody or shorter isoforms that are transcribed/translated from exons at the 5′ end of the gene, not affected by the premature stop codon in exon 7. These results paralleled the findings in *Disc1*^{Tm1Kara} mice (Kvajo et al. 2008).

Examination of the gross brain morphology of *Disc1* mutant mice

Reduced cortical thickness and enlarged lateral ventricles have been reported in patients with schizophrenia (Brown et al. 1986). In *Disc1* mutant mice, the thicknesses of the cerebral cortex and corpus callosum and the volume of the lateral ventricle were measured (Fig. 2a). Unlike some patients with schizophrenia, the thicknesses of the cortex and corpus callosum were not altered in Het and Homo mice (Fig. 2b, c). However, the sizes of the lateral ventricle in Het and Homo mice were enlarged compared to WT (Fig. 2d). These data are consistent with that of other *Disc1* mutant mice models (Hikida et al. 2007; Pletnikov et al. 2008; Shen et al. 2008) and patients with schizophrenia (Brown et al. 1986).

Behavioral phenotypes of *Disc1* mutant mice

In the elevated plus maze test, no significant differences were noted among the three genotypes in the times spent in the open arms, closed arms, and the central region (Fig. 3a). In the forced swim test, no significant differences in the time spent in immobility, swimming and struggle among the three genotypes were found (Fig. 3b). We next examined learning and memory abilities. In the novel object recognition test, again, all three groups of mice spent a greater amount of time exploring the novel object, indicating that with proper short-term memory, they all successfully distinguished the novel object from the familiar one (Fig. 3c). The Y-maze test was conducted to estimate spatial memory. All three groups travelled greater distances in the novel arm, meaning that they all successfully distinguished the novel arm from the start and familiar arms using short-term spatial memory (Fig. 3d). In the water maze test, all mice also exhibited comparable levels of learning effectiveness, as the time spent in finding the hidden platform was significantly shortened in each case (Fig. 3e). In the probe test (Fig. 3f), while the hidden platform was removed, all mice still spent more time in the quadrant in which the platform was formerly located (P) compared to other quadrants (NP), indicating that the memory of previous training sessions was still present in all three groups of mice.
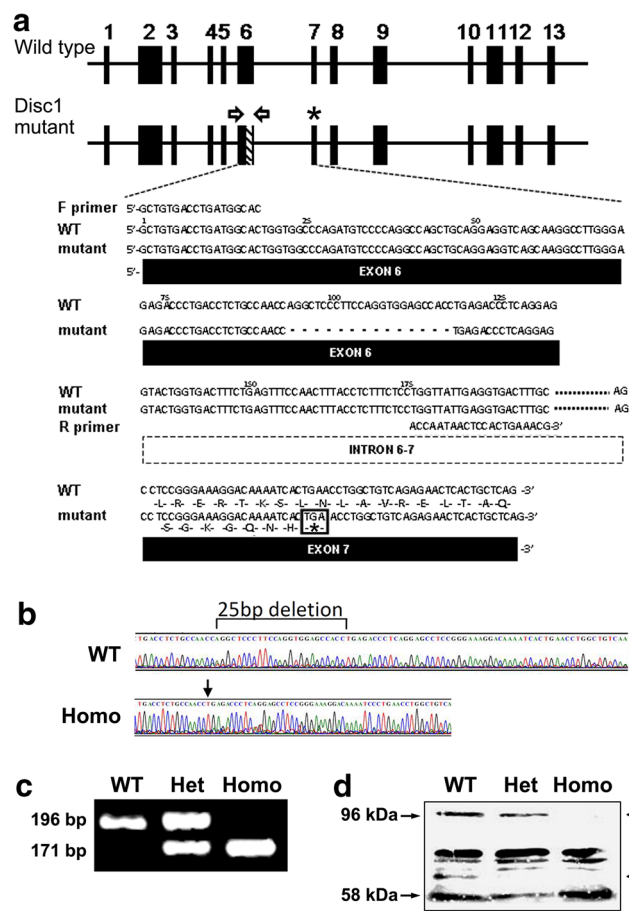
Fig. 1 Generation of *Disc1* mutant mice in the C57BL/6J genetic background. **a** Genomic structure of the mouse Disc1 gene. The position of the 129S6/SvEv deletion polymorphism in exon 6 of C57BL/6J mice is indicated by a *hatched bar*. The *asterisk* indicates the presence of a premature stop codon in exon 7. *White arrowheads* indicate the position of the PCR primers used. Genomic DNA sequences of exon 6 for both wild-type and *Disc1* mutant mice are shown, and the sequences of the forward and reverse primer set are also displayed. **b** The truncated transcript of a 25-bp deletion of the 129S6/SvEv Disc1 allele was confirmed by cDNA sequencing. **c** A truncated DNA fragment (171 bp) was revealed in Disc1 homozygous mutant mice, whereas an intact DNA fragment (196 bp) was identified in WT mice. **d** Disc1 protein expression revealed by immunoblotting. A 100 kDa Disc1 isoform (*arrowhead*) was absent in Homo mice and significantly reduced in Het mice while a 70 kDa band (*arrowhead*) was not detected in Homo and largely reduced in Het mice. However, many Disc1 isoforms were still expressed in all three genotypes. WT, wild-type; Het, *Disc1* heterozygous mutant; Homo, *Disc1* homozygous mutant

Patients with schizophrenia behave inadequately in the working memory test (Goldman-Rakic 1994); thus, the working memory in *Disc1* mutant mice was examined using the delayed non-match recognition task (Fig. 4). During the training phase, most WT mice easily learned the rules of this test, resulting in a higher (>80 %) passing percentage after 3 days of training. However, in Het mice, the passing rate was approximately 60 %. In contrast, the

passing rate was <40 % in Homo mice (Fig. 4a). After an extended training period (for WT, 3.1 days; Het, 3.5 days; Homo, 3.9 days), all mice learned the rules of the test with a passing rate >80 %. In the testing phase, all mice performed equally well when the delay time was short (i.e., 5, 15 and 30 s). However, when the delay time extended to 45 and 60 s, Het and Homo mice were unable to make correct choices (Fig. 4b). These results demonstrate the impairment of working memory in *Disc1* mutant mice, which is similar to other *Disc1* mutant mice (Li et al. 2007; Kvajo et al. 2008; Niwa et al. 2010) and patients with schizophrenia (Goldman-Rakic 1994).

Dendritic structure of layer II/III pyramidal neurons in the mPFC

In rodents, the mPFC is important for working memory (Castner et al. 2004) and is functionally equivalent to the dorsolateral prefrontal cortex (DLPFC) in humans (Moghaddam and Homayoun 2008), in which an altered dendritic structure has been reported in patients with schizophrenia. Consequently, the cytoarchitecture of the mPFC in *Disc1* mutant mice was characterized. The dendritic trees of Golgi-stained layer II/III pyramidal neurons in the mPFC were three-dimensionally reconstructed (Fig. 5a, b). In apical dendrites, the complexity (revealed by Sholl analysis, Fig. 5c), arborization (measured by the number of segments in each order, Fig. 5d), and dendritic length (Fig. 5g) were significantly reduced in Homo mice. The total number of bifurcation and segments was affected in both apical and basilar dendrites (Fig. 5d, f). However, compared to WT mice, these features in mPFC neurons of Het mice did not change much. The lengths of the intermodal and terminal segments were comparable between three genotypes in both apical and basilar dendrites (Fig. 5h, i). Together, these results suggested a role for Disc1 in the arborization, but not elongation, of dendritic branches.

The dendritic morphology of Golgi-stained layer II/III pyramidal mPFC neurons at higher magnifications was also examined. For the apical dendrites, the density of dendritic spines and the dendritic diameter of the trunk (T) and collaterals (C) in the proximal (<50 μm from soma) and distal (bifurcation near the surface) regions were quantified, respectively (Fig. 6a). For the basilar dendrites, the spine density and dendritic diameter were measured in the dendritic segments of the primary to the fourth-order dendrites (Fig. 6b). Compared to WT, reduced spine density was noted in Het and Homo mice in both proximal (Fig. 6c) and distal (Fig. 6d) regions of the apical dendrites. However, in basilar dendrites, decreased spine density was noted only in dendritic segments from Homo mice (Fig. 6e). Notably, reduced dendritic diameter was
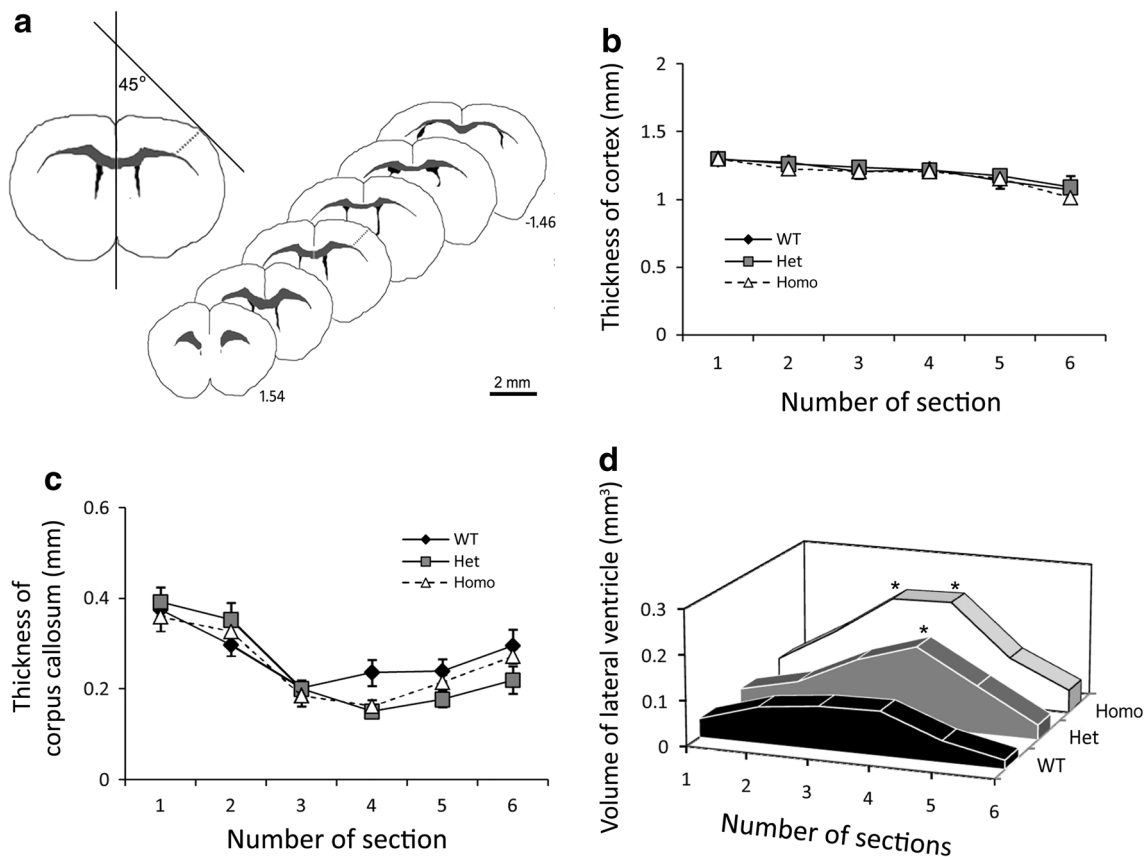
Fig. 2 Overall brain structure. **a** The thickness of cortex was measured from the surface to the white matter of the cortex at the point which is tangent to the surface by a imaginary line 45° deviated from the midline. The corpus callosum and lateral ventricles are marked in the schema. *Numbers* indicate the distance from the bregma (mm). The interval between the two sections is about 500 μm. **b–d** Morphological features, including the thickness of the cortex (**b**), the thickness of the corpus callosum (**c**), and the volume of the lateral ventricle (**d**), were measured. Enlarged lateral ventricles were observed in both Het and Homo groups, while the thickness of the cortex and corpus callosum were not altered in Disc1 mutants. Data are expressed as the mean ± SEM. *Asterisks* indicate significant differences when comparing with WT (*$p < 0.05$)

observed in both apical (Fig. 6f, g) and basilar (Fig. 6h) dendrites in Het and Homo mice.

Changes in the intrinsic and synaptic properties of mPFC neurons in Disc1 mutant mice

To further elucidate the physiological properties of layer II/III pyramidal mPFC neurons in Disc1 mutant mice, we performed whole-cell patch-clamp recording using brain slices prepared from adult (8- to 12-week-old) male mice. We first characterized the intrinsic properties, including resting membrane potential (V_m), input resistance (R_{in}), time constant (τ) and capacitance (C), along with the properties of the AP by current injections. The V_m in Het and Homo mice was more negative relative to that in WT mice (Table 1). However, the R_{in} in both Het and Homo was smaller than that in WT (Fig. 7c), and the τ and C were not distinguishable between the three genotypes (Table 1).

For the AP properties, the thresholds for generating AP were more positive in Het and Homo mice than in WT mice. Together with the more negative V_m, the increased AP threshold suggested that more positive currents were required for AP initiation, resulting in decreased excitability in layer II/III pyramidal mPFC neurons in *Disc1* mutant mice. For a single AP, both the amplitude and width were decreased in Het and Homo mice, whereas the AHP was unchanged (Table 1).

With supra-threshold current injections, AP trains were instigated (Fig. 7a). The responses (AP) to injected currents were plotted as an AP frequency-injected current (F–I) curve (Fig. 7b). Compared to WT mice, the F–I curve was shifted rightward in both Het and Homo mice, indicating the reduction of neuronal excitability (Liao and Lee 2012). This reduced excitability in Het and Homo mice might be explained by the decreased R_{in} (Fig. 7c).

The synaptic properties of layer II/III pyramidal mPFC neurons were also examined. The sEPSCs were recorded,
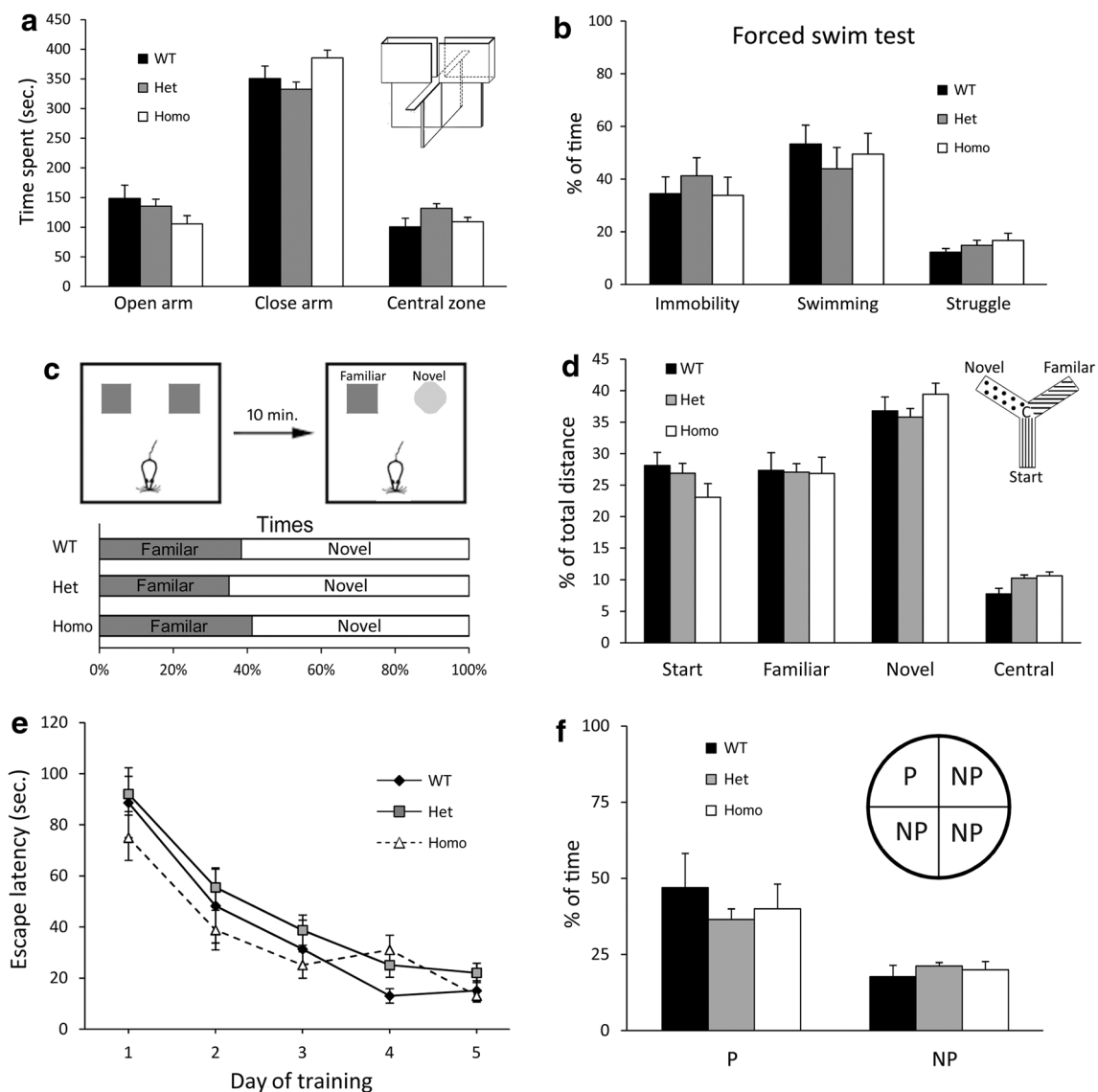
Fig. 3 Behavioral tests in *Disc1* mutant mice. **a** Elevated plus maze. The time spent in the open arm, closed arm and central zone was quantified. No differences were identified among the three genotypes. **b** Forced swim test. The time spent in immobility, swimming and struggle was measured; however, no significant differences were noted among the three genotypes. **c** Novel object recognition task. All three groups of mice spent more time exploring the novel object than the familiar one. **d** Y-maze for spatial memory. All three genotypes of

mice travelled the greatest distance in the novel arm of the maze. **e** The learning phase of the Morris water maze. The latency from the release of the animal to its location of the platform was decreased in all three genotypes of mice. **f** The testing phase of the Morris water maze. All mice of the three genotypes spent more time in the quadrant in which the platform was located. *P* platform, *NP* non-platform, average of three non-platform quadrants. Data are expressed as the mean ± SEM

and both frequency and amplitude were analyzed (Fig. 7d). Surprisingly, the sEPSC frequencies were comparable among the three genotypes, while greater amplitude was observed only in neurons from Homo mice. Given the density of dendritic spines, the major receiving sites of excitatory neurotransmission were reduced in neurons of both Het and Homo mice. As such, reduced EPSC frequency was expected. However, the frequency was not changed in *Disc1* mutant mice, suggesting a compensatory mechanism that may counterbalance the reduction of

dendritic spines. To test whether the release of excitatory neurotransmitters from the presynaptic terminals was changed, the paired-pulse ratio (PPR), which is negatively correlated with the release probability (Zucker and Regehr 2002), was examined. To determine the PPR, paired stimuli were delivered at fixed 50-ms intervals. The PPR of neurons in WT mice was approximately 2, indicating a low-release type of synapse. In the case of Homo, the PPR was significantly smaller than that of WT, suggesting a high-release synaptic property. For Het, the PPR was also
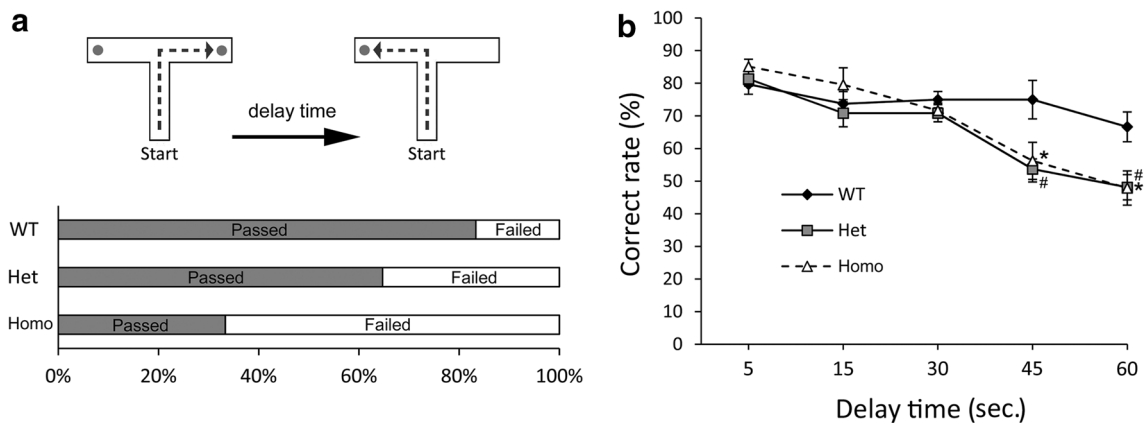
Fig. 4 Impaired working memory in *Disc1* mutant mice. The working memory of mice was estimated in the delayed non-match to place task. **a** The pass rate after the first three-day training period. **b** In the testing phase, all mice exhibited a greater correct rate when the delay time was short (5, 15, 30 s). However, both Het and Homo mice exhibited low correct rates ($\sim$50 %) when the delay time was prolonged to 45 and 60 s, whereas WT exhibited a greater correct rate when the delay was extended to 45 and 60 s. Data are expressed as the mean $\pm$ SEM. *Hash symbols and asterisks* indicate that there are significant differences when comparing WT to Het and WT to KO, respectively (#, *$p < 0.05$)

smaller than that of WT; however, statistical significance was not achieved (Fig. 7e).

Discussion

Our results revealed the behavioral, morphological and physiological phenotypes of a *Disc1* mutant mouse model in which the 129S6/SvEv variant of the *Disc1* gene was transferred into the C57BL/6J mouse strain. Our cDNA sequencing data confirmed the deletion of 25 bp within exon 6 of the *Disc1* gene and a premature termination in exon 7 (Koike et al. 2006). In both heterozygous and homozygous *Disc1* mutant (Het and Homo) mice, enlarged lateral ventricles, reduced dendritic diameter, spine density and excitability in layer II/III mPFC neurons were observed, which may lead to impaired mPFC-mediated working memory function in these mice.

Brain imaging techniques have identified structural and functional changes in patients with schizophrenia (Meyer-Lindenberg 2010). Studies show that overall gray matter, white matter and whole brain volumes are decreased, while the volume of the ventricle is increased in schizophrenia subjects (Brown et al. 1986; Ellison-Wright et al. 2008). In the *Disc1* mutant mice of this study, enlarged lateral ventricles were observed, while the thicknesses of somatosensory cortex and corpus callosum exhibited no significant differences compared to WT mice. Several postmortem brain studies have shown reduced volume in subcortical regions such as thalamus and striatum (Byne et al. 2001; Danos et al. 2003; Kreczmanski et al. 2007). The enlarged lateral ventricle in *Disc1* Het and Homo knockout mice may be resulted from the reduction of volumes in thalamus or striatum. Alternatively, greater changes in brain structure usually occur in chronic schizophrenia (Ellison-Wright et al. 2008). More severe changes of brain structures in *Disc1* mutant mice of older ages might be expected.

Working memory is a prefrontal cortex-mediated cognitive function and is commonly impaired among patients with schizophrenia (Goldman-Rakic 1994; Hennah et al. 2005; Volk and Lewis 2010). Based on postmortem brain studies, reduced dendritic complexity and spine density in layer III DLPFC pyramidal neurons have been linked to a reduction in working memory among schizophrenia patients (Glantz and Lewis 2000; Kolluri et al. 2005). In rodents, the function of mPFC is analogous to that of the DLPFC in humans (Moghaddam and Homayoun 2008). Our morphological observations of dendritic architecture in layer II/III mPFC neurons in Homo mice, including reduced dendritic complexity, length and spine density, match findings in human patients with schizophrenia (Glantz and Lewis 2000). This specific cognitive impairment in *Disc1* mutants (both Het and Homo) is also consistent with that in *Disc1^{Tm1Kara}* mice (Koike et al. 2006; Kvajo et al. 2008). Owing to a similar genetic background, reduced dendritic branches and diameter in layer II/III pyramidal neurons in the mPFC of Homo mice in the present study would possibly account for the volumetric reduction ($\sim$14 %) in the mPFC of Homo *Disc1^{Tm1Kara}* mice (Kvajo et al. 2008).

The functions of the DISC1 protein in the nervous system have been extensively investigated. The DISC1 protein interacts with various cytoskeleton and synaptic scaffolding proteins and plays roles in regulating neurites and spines (Le Strat et al. 2009; Hayashi-Takagi et al. 2010). Therefore, mutations of *Disc1* would affect the
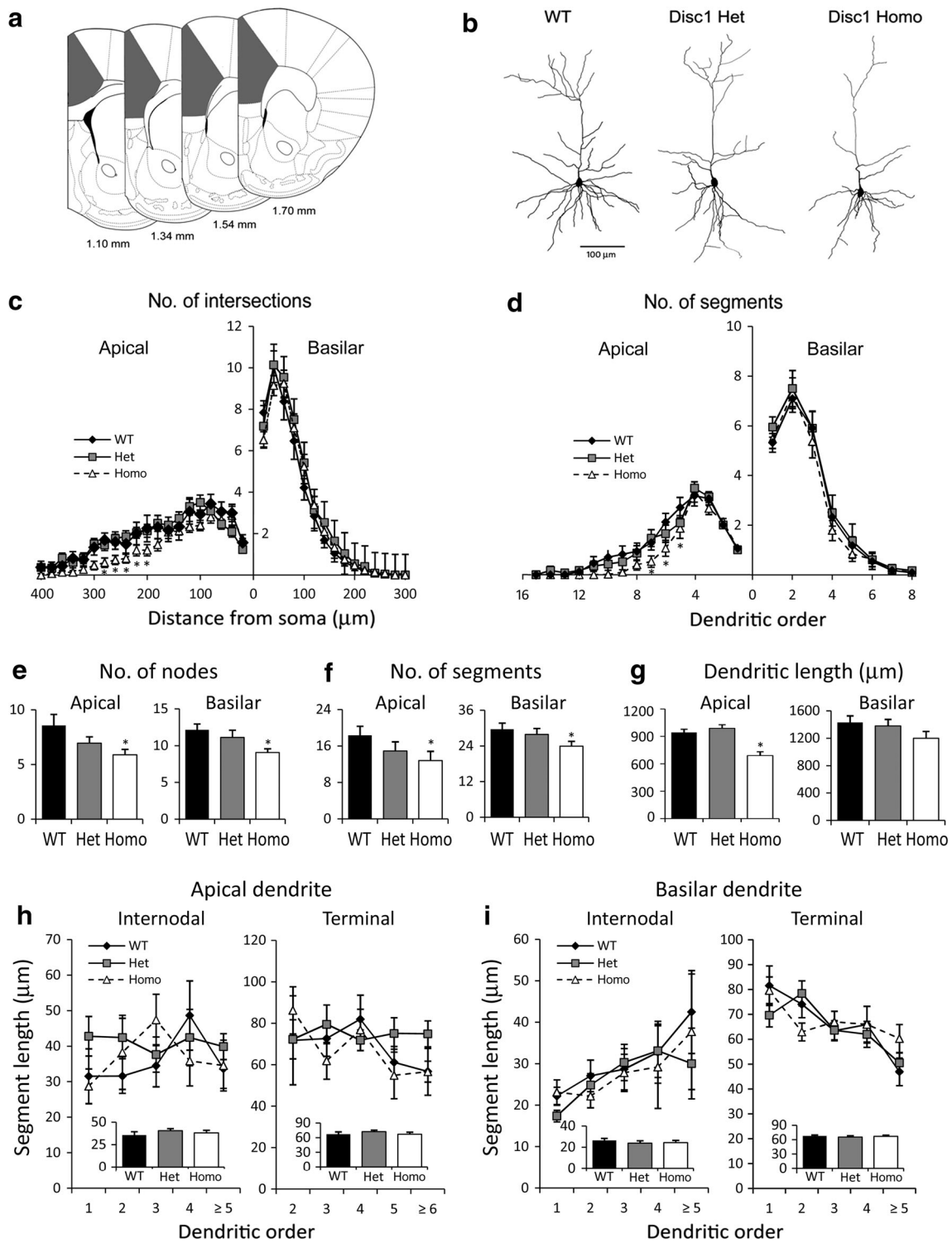
Fig. 5 Dendritic complexity of layer II/III pyramidal mPFC neurons. a The mPFC is marked in gray in the coronal sections of a mouse brain. *Numbers* indicate the distance from the bregma (mm). b Examples of Golgi–Cox-impregnated pyramidal neurons were obtained from layer II/III of the mPFC. The complexity of the branching pattern in apical and basilar dendrites of mPFC neurons was examined by Sholl's concentric ring method (c) and the number of segments in different orders (d). The total number of bifurcation nodes (e), segments (f) and the dendritic length (g) were also quantified. The lengths of the internodal and terminal segments were measured in apical (h) and basilar (i) dendrites. Data are expressed as the mean ± SEM. *Asterisks* indicate significant differences (*p < 0.05)
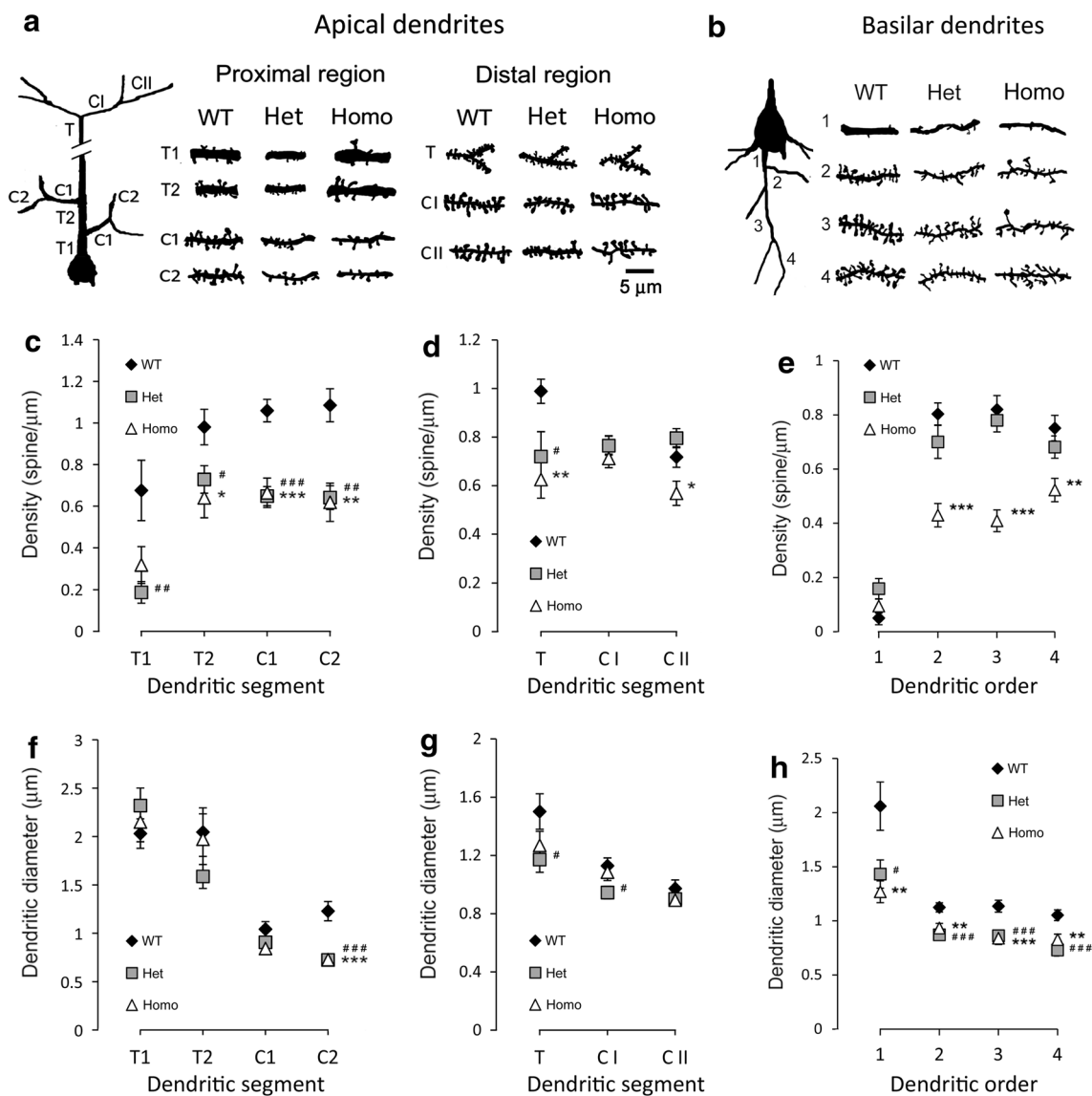
Fig. 6 Dendritic features of layer II/III pyramidal mPFC neurons. Schematic representation of dendritic fragments in apical (**a**) and basilar (**b**) dendrites of layer II/III mPFC pyramidal neurons. In the apical dendrites, fragments were collected from the trunk (T) and collaterals (C) from the proximal (<50 μm from soma) and distal (bifurcation near the surface) regions, respectively. In the basilar dendrites, fragments were classified by dendritic order. Densities of the dendritic spines in the proximal region (**c**) and distal region (**d**) of the apical dendrite and various dendritic orders of the basilar dendrites (**e**) are shown. Dendritic diameter in the proximal region (**f**) and distal region (**g**) of the apical dendrite and various dendritic orders of the basilar dendrites (**h**) are plotted. Data are expressed as the mean ± SEM. *Hash symbols and asterisks* indicate that there are significant differences when comparing WT to Het and WT to KO, respectively ($^{\#}$, $^{*}p < 0.05$; $^{\#\#}$, $^{**}p < 0.01$; $^{\#\#\#}$, $^{***}p < 0.001$)

Table 1 Intrinsic properties of layer II/III pyramidal neurons in the mPFC

	V_m (mV)	τ (ms)	C (pF)	Thre (mV)	Amp (mV)	W_h (ms)	AHP (mV)
WT	−69.6 ± 0.9	10.2 ± 0.5	79.2 ± 5.4	−43.6 ± 0.7	90.4 ± 0.7	1.70 ± 0.07	−2.25 ± 0.45
Het	−73.0 ± 1.2*	11.4 ± 0.7	87.7 ± 5.9	−40.2 ± 1.2*	86.4 ± 0.8***	1.40 ± 0.06**	−2.95 ± 0.35
Homo	−72.5 ± 1.0*	10.6 ± 1.1	87.6 ± 6.4	−41.6 ± 1.3	85.1 ± 1.5**	1.45 ± 0.05**	−3.51 ± 0.96

Values are mean ± SEM

V_m resting membrane potential, τ time constant, C capacitance, *Thre* threshold of action potential (AP), *Amp* amplitude of AP, W_h half width of AP, *AHP* amplitude of afterhyperpolarization

* $p < 0.05$, ** $p < 0.01$. *** $p < 0.001$ significant difference comparing with WT. Student's *t* test
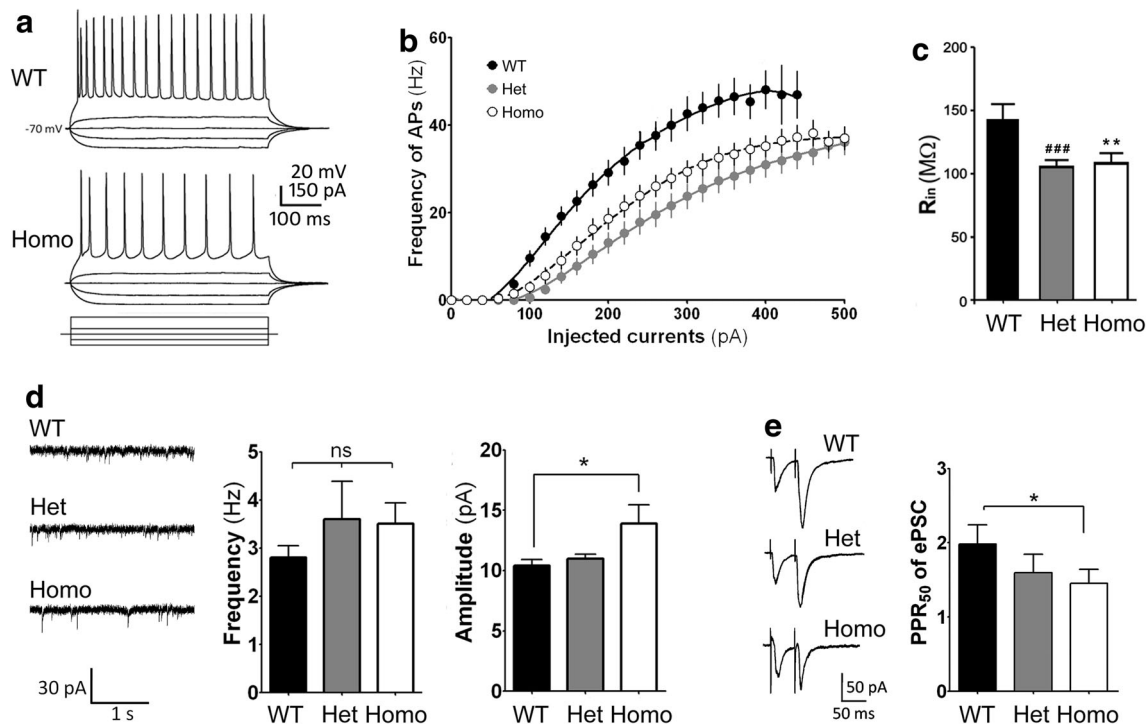
Fig. 7 Intrinsic and synaptic properties of layer II/III pyramidal mPFC neurons. **a** In the mPFC neurons of both WT and Homo mice, an action potential (AP) train can be induced by current injections. **b** The frequency of APs was plotted against the amount of injected currents (F–I relationship). **c** The input resistance (R_{in}) of mPFC neurons was compared in WT, Het and Homo mice. **d** Examples of spontaneous excitatory postsynaptic currents (sEPSCs) recorded in the mPRC neurons of WT, Het and Homo mice are illustrated. The frequency and amplitude of sEPSCs were analyzed. **e** Responses of paired-pulse stimuli in mPFC neurons are shown. In the Homo group, the paired-pulse ratio (PPR) was less than that of WT mice. Data are expressed as the mean ± SEM. *Asterisks* indicate significant differences when comparing with WT (*$p < 0.05$; **$p < 0.01$; ***$p < 0.001$)

dendritic architecture in Het and Homo mice, as observed in this study and in other *Disc1* mutant mouse models (Li et al. 2007; Kvajo et al. 2008, 2011; Pletnikov et al. 2008; Niwa et al. 2010; Ayhan et al. 2011).

In addition to morphological changes in mPFC neurons, our results also revealed alterations in the physiological aspect. First, the excitability of mPFC neurons declined in both Het and Homo mice. This is most likely due to a decrease in R_{in} (Nataraj et al. 2010; Liao and Lee 2012). The neuronal excitability and R_{in} are reduced in the granule cells of the dentate gyrus of Homo *Disc1^{Tm1Kara}* mice (Kvajo et al. 2011), indicating a Disc1-related regulatory mechanism for R_{in} and neuronal excitability. The decrease in R_{in} might be attributed to an increase in soma size (Golowasch et al. 2009). However, that is not likely to be the case, as the size and membrane capacitance of recorded neurons in the Homo mice in this study and in Homo *Disc1^{Tm1Kara}* mice were not different from those of WT mice (Kvajo et al. 2011). In various CNS neurons, R_{in} is modulated by the kinetics of ion channels, such as hyperpolarization-activated cyclic nucleotide-gated (HCN) channels (Robinson and Siegelbaum 2003). It is also known that the DISC1 protein interacts with phosphodiesterase 4 (PDE4) (Millar et al. 2005), which degrades

intracellular cAMP. In Homo *Disc1^{Tm1Kara}* mice, the activity of PDE4 is disrupted, and consequently, the cAMP level is elevated (Kvajo et al. 2011). Thus, the reduced neuronal excitability in these mice might result from the opening of cAMP-specific HCN channels. HCN channels are also highly expressed in the mPFC (Li et al. 2010). Elevated cAMP level and greater opening probability of HCN might explain the reduced neuronal excitability in our Disc1 model. Besides, GSK-3β, a DISC1 binding partner (Mao et al. 2009), modulates the activity of voltage-gated M-type potassium channels (Kapfhamer et al. 2010) which might play roles in modulating R_{in} and neuronal excitability (Santini and Porter 2010). However, it is not clear if the expression or activity of GSK-3β is altered in the mPFC of our *Disc1* mutant mice. On the other hand, reduction in neuronal excitability might be a compensatory mechanism elicited by the over-activation of neural circuit. Nonetheless, further electrophysiological validation is warranted.

In addition to intrinsic membrane properties such as R_{in}, neuronal excitability is also determined by synaptic transmission by the way of synaptic efficacy (Spruston 2008). Given that dendrites are the major receiving sites of synaptic inputs, reductions in dendritic complexity, diameter

and spine density suggest a decline of synaptic efficacy (Komendantov and Ascoli 2009). However, our results indicated that the frequency of sEPSCs in mPFC neurons of *Disc1* mutant mice is comparable to that in WT mice. Therefore, we suggest an increase of presynaptic transmitter release as a compensatory mechanism elicited in Homo mice.

The reduction of PPR in mPFC neurons of Homo mice supports this idea. Usually, the release probability is negatively correlated with PPR (Zucker and Regehr 2002). With lesser PPR or greater release probability, the frequency of sEPSC in mPFC neurons of Homo mice is adjusted to WT levels, even though the spine density has been reduced. In the meantime, increased sEPSC amplitude in Homo groups is evident. However, the mPFC neurons in Het mice exhibit moderate structural abnormalities, as the compensatory mechanism is most likely not as significant as that in Homo mice. The PPR is not reduced in mPFC neurons in Het mice, and the amplitude of sEPSCs is not altered.

Due to the moderate structural abnormalities in Het mice and feasible compensatory mechanisms elicited in Homo mice, both genotypes performed comparably to WT mice in most of the behavioral tests, including the delayed non-match recognition task with low working memory loads (short delay time). In patients with schizophrenia, reduced PFC activity and impaired function are noted, particularly when the working memory load is high (Manoach 2003; Tan et al. 2007). This phenomenon is clearly replicated in this mouse model and in $Disc1^{Tm1Kara}$ mice (Koike et al. 2006; Kvajo et al. 2008). In both mouse lines, Het and Homo mice displayed significant declines in the working memory test as the delay time (working memory load) increased. In these mice, the structural and functional deficits (with compensatory mechanisms) do not largely impair, but rather limit the cognitive capacity.

In the present *Disc1* mouse model, relatively limited yet specific behavioral abnormalities, working memory deficits, were observed compared to other *Disc1* mouse models. In dominant-negative transgenic *Disc1* mice, for example, impaired emotion-related behaviors and sociability are often observed (Hikida et al. 2007; Li et al. 2007; Pletnikov et al. 2008; Shen et al. 2008; Ayhan et al. 2011). These inconsistent and widespread deficits generated by different genetic manipulations reflect the complexity of DISC1 interactome (Camargo et al. 2007) and undetermined compensatory mechanisms while different isoforms are affected. However, different genetic manipulations have different validity in reflecting genuine disease mechanisms. In mice carrying truncated DISC1 or c-terminal fragment, impaired neural development and abnormal behaviors are observed, yet exogenous expression of dominant-negative proteins does not simulate the condition

of chromosomal abnormality in the Scottish pedigree nor the genetic variants in patients with schizophrenia or schizoaffective disorders (Brandon and Sawa 2011). For the development of therapeutic strategy for major psychiatric disorders, such as schizophrenia, humanized animal models replicating authentic disease situation are needed.

In $Disc1^{Tm1Kara}$ mice and our *Disc1* mutants, the breakpoint in *Disc1* gene mimicked that in the Scottish family. Besides, the relatively specific deficits in working memory in these mutants might represent a good model for schizophrenia (Goldman-Rakic 1994; Castner et al. 2004), while other indiscriminate effects on cognition reflect more severe problems typically found in mental retardation and other neurodevelopmental disorders (Arguello and Gogos 2012). On the other hand, the behavioral phenotypes in our model might represent subjects in the prodromal states of psychosis, in which predominant symptoms are not yet manifested. More severe behavioral changes might be expected in older *Disc1* mutant mice or in conjunction with environmental insults. The interplays and consequences of genetic and environmental factors in the pathogenesis of mental disorders such as schizophrenia (Abazyan et al. 2010; Ibi et al. 2010) could be further investigated using this *Disc1* mutant model.

In the Scottish family mentioned previously, a balanced t(1:11)(q42.1:q14.3) chromosomal translocation was highly associated with the manifestation of various mental disorders, including schizophrenia (Millar et al. 2000; Blackwood et al. 2001). Number of pathogenic mechanisms of DISC1 disruption in mental disorders has been suggested such as haploinsufficiency (Camargo et al. 2007), C-terminal truncation (Kamiya et al. 2005) and chimeric fusion proteins (Zhou et al. 2008, 2010; Eykelenboom et al. 2012). In our Homo mice, a premature stop codon is in exon 7, indicating a loss of C-terminus of Disc1 protein. Our findings in Het mice also support the model of haploinsufficiency. However, the adverse effects of chimeric fusion proteins cannot be examined in the present mutants. It is a limit of this animal model. Novel knock-in models expressing chimeric fusion proteins should be generated and the pathogenic mechanism of Scottish DISC1 translocation might be revealed.

The phenotypic features of our Het mice illustrate that only one copy of truncated *Disc1* gene can induce significant alternations in neuronal excitability, dendritic diameter and behavior in mice. Not only in 129S6/SvEv strain, 25-bp deletion in exon 6 of *Disc1* gene has been demonstrated in all 129 mouse substrains and embryonic stem (ES) cell lines derived from 129 substrains (Clapcote and Roder 2006). In the past years, most of the knockout mice were generated from 129 substrain-derived ES cells and the 129 *Disc1* variant might be carried especially the target gene and *Disc1* are in the same chromosome (8). In such

cases, genotyping for *Disc1* is advised. For 129 *Disc1* variant carriers, performance of working memory as well as neuronal excitability and dendritic architecture in mPFC neurons might have to be examined.

References

Abazyan B, Nomura J, Kannan G, Ishizuka K, Tamashiro KL, Nucifora F, Pogorelov V, Ladenheim B, Yang C, Krasnova IN, Cadet JL, Pardo C, Mori S, Kamiya A, Vogel MW, Sawa A, Ross CA, Pletnikov MV (2010) Prenatal interaction of mutant DISC1 and immune activation produces adult psychopathology. Biol Psychiatry 68:1172–1181

Arguello PA, Gogos JA (2012) Genetic and cognitive windows into circuit mechanisms of psychiatric disease. Trends Neurosci 35:3–13

Ayhan Y, Abazyan B, Nomura J, Kim R, Ladenheim B, Krasnova IN, Sawa A, Margolis RL, Cadet JL, Mori S, Vogel MW, Ross CA, Pletnikov MV (2011) Differential effects of prenatal and postnatal expressions of mutant human DISC1 on neurobehavioral phenotypes in transgenic mice: evidence for neurodevelopmental origin of major psychiatric disorders. Mol Psychiatry 16:293–306

Blackwood DH, Fordyce A, Walker MT, St Clair DM, Porteous DJ, Muir WJ (2001) Schizophrenia and affective disorders—cosegregation with a translocation at chromosome 1q42 that directly disrupts brain-expressed genes: clinical and P300 findings in a family. Am J Hum Genet 69:428–433

Brandon NJ, Sawa A (2011) Linking neurodevelopmental and synaptic theories of mental illness through DISC1. Nat Rev Neurosci 12:707–722

Brown R, Colter N, Corsellis JA, Crow TJ, Frith CD, Jagoe R, Johnstone EC, Marsh L (1986) Postmortem evidence of structural brain changes in schizophrenia. Differences in brain weight, temporal horn area, and parahippocampal gyrus compared with affective disorder. Arch Gen Psychiatry 43:36–42

Byne W, Buchsbaum MS, Kemether E, Hazlett EA, Shinwari A, Mitropoulou V, Siever LJ (2001) Magnetic resonance imaging of the thalamic mediodorsal nucleus and pulvinar in schizophrenia and schizotypal personality disorder. Arch Gen Psychiatry 58:133–140

Camargo LM, Collura V, Rain JC, Mizuguchi K, Hermjakob H, Kerrien S, Bonnert TP, Whiting PJ, Brandon NJ (2007) Disrupted in Schizophrenia 1 Interactome: evidence for the close connectivity of risk genes and a potential synaptic basis for schizophrenia. Mol Psychiatry 12:74–86

Castner SA, Goldman-Rakic PS, Williams GV (2004) Animal models of working memory: insights for targeting cognitive dysfunction in schizophrenia. Psychopharmacology 174:111–125

Clapcote SJ, Roder JC (2006) Deletion polymorphism of Disc1 is common to all 129 mouse substrains: implications for gene-targeting studies of brain function. Genetics 173:2407–2410

Danos P, Baumann B, Krämer A, Bernstein HG, Stauch R, Krell D, Falkai P, Bogerts B (2003) Volumes of association thalamic nuclei in schizophrenia: a postmortem study. Schizophr Res 60:141–155

Ellison-Wright I, Glahn DC, Laird AR, Thelen SM, Bullmore E (2008) The anatomy of first-episode and chronic schizophrenia: an anatomical likelihood estimation meta-analysis. Am J Psychiatry 165:1015–1023

Eykelenboom JE, Briggs GJ, Bradshaw NJ, Soares DC, Ogawa F, Christie S, Malavasi EL, Makedonopoulou P, Mackie S, Malloy MP, Wear MA, Blackburn EA, Bramham J, McIntosh AM, Blackwood DH, Muir WJ, Porteous DJ, Millar JK (2012) A t(1;11) translocation linked to schizophrenia and affective disorders gives rise to aberrant chimeric DISC1 transcripts that encode structurally altered, deleterious mitochondrial proteins. Hum Mol Genet 21:3374–3386

Franklin K, Paxinos G (2008) The mouse brain in stereotaxic coordinates. Academic Press, New York

Glantz LA, Lewis DA (2000) Decreased dendritic spine density on prefrontal cortical pyramidal neurons in schizophrenia. Arch Gen Psychiatry 57:65–73

Goldman-Rakic PS (1994) Working memory dysfunction in schizophrenia. J Neuropsychiatry Clin Neurosci 6:348–357

Golowasch J, Thomas G, Taylor AL, Patel A, Pineda A, Khalil C, Nadim F (2009) Membrane capacitance measurements revisited: dependence of capacitance value on measurement method in nonisopotential neurons. J Neurophysiol 102:2161–2175

Hayashi-Takagi A, Takaki M, Graziane N, Seshadri S, Murdoch H, Dunlop AJ, Makino Y, Seshadri AJ, Ishizuka K, Srivastava DP, Xie Z, Baraban JM, Houslay MD, Tomoda T, Brandon NJ, Kamiya A, Yan Z, Penzes P, Sawa A (2010) Disrupted-in-Schizophrenia 1 (DISC1) regulates spines of the glutamate synapse via Rac1. Nat Neurosci 13:327–332

Hennah W, Tuulio-Henriksson A, Paunio T, Ekelund J, Varilo T, Partonen T, Cannon TD, Lönnqvist J, Peltonen L (2005) A haplotype within the DISC1 gene is associated with visual memory functions in families with a high density of schizophrenia. Mol Psychiatry 10:1097–1103

Hikida T, Jaaro-Peled H, Seshadri S, Oishi K, Hookway C, Kong S, Wu D, Xue R, Andrade M, Tankou S, Mori S, Gallagher M, Ishizuka K, Pletnikov M, Kida S, Sawa A (2007) Dominant-negative DISC1 transgenic mice display schizophrenia-associated phenotypes detected by measures translatable to humans. Proc Natl Acad Sci USA 104:14501–14506

Ibi D, Nagai T, Koike H, Kitahara Y, Mizoguchi H, Niwa M, Jaaro-Peled H, Nitta A, Yoneda Y, Nabeshima T, Sawa A, Yamada K (2010) Combined effect of neonatal immune activation and mutant DISC1 on phenotypic changes in adulthood. Behav Brain Res 206:32–37

Ishizuka K, Kamiya A, Oh EC, Kanki H, Seshadri S, Robinson JF, Murdoch H, Dunlop AJ, Kubo K, Furukori K, Huang B, Zeledon M, Hayashi-Takagi A, Okano H, Nakajima K, Houslay MD, Katsanis N, Sawa A (2011) DISC1-dependent switch from progenitor proliferation to migration in the developing cortex. Nature 473:92–96

Jaaro-Peled H, Hayashi-Takagi A, Seshadri S, Kamiya A, Brandon NJ, Sawa A (2009) Neurodevelopmental mechanisms of schizophrenia: understanding disturbed postnatal brain maturation through neuregulin-1-ErbB4 and DISC1. Trends Neurosci 32:485–495

Kamiya A, Kubo K, Tomoda T, Takaki M, Youn R, Ozeki Y, Sawamura N, Park U, Kudo C, Okawa M, Ross CA, Hatten ME, Nakajima K, Sawa A (2005) A schizophrenia-associated mutation of DISC1 perturbs cerebral cortex development. Nat Cell Biol 7:1167–1178

Kapfhamer D, Berger KH, Hopf FW, Seif T, Kharazia V, Bonci A, Heberlein U (2010) Protein phosphatase 2a and glycogen synthase kinase 3 signaling modulate prepulse inhibition of the acoustic startle response by altering cortical M-type potassium channel activity. J Neurosci 30:8830–88340

Koike H, Arguello PA, Kvajo M, Karayiorgou M, Gogos JA (2006) Disc1 is mutated in the 129S6/SvEv strain and modulates

working memory in mice. Proc Natl Acad Sci USA 103: 3693–3697

Kolluri N, Sun Z, Sampson AR, Lewis DA (2005) Lamina-specific reductions in dendritic spine density in the prefrontal cortex of subjects with schizophrenia. Am J Psychiatry 162:1200–1202

Komendantov AO, Ascoli GA (2009) Dendritic excitability and neuronal morphology as determinants of synaptic efficacy. J Neurophysiol 101:1847–1866

Kreczmanski P, Heinsen H, Mantua V, Woltersdorf F, Masson T, Ulfig N, Schmidt-Kastner R, Korr H, Steinbusch HW, Hof PR, Schmitz C (2007) Volume, neuron density and total neuron number in five subcortical regions in schizophrenia. Brain 130:678–692

Kvajo M, McKellar H, Arguello PA, Drew LJ, Moore H, MacDermott AB, Karayiorgou M, Gogos JA (2008) A mutation in mouse Disc1 that models a schizophrenia risk allele leads to specific alterations in neuronal architecture and cognition. Proc Natl Acad Sci USA 105:7076–7081

Kvajo M, McKellar H, Drew LJ, Lepagnol-Bestel AM, Xiao L, Levy RJ, Blazeski R, Arguello PA, Lacefield CO, Mason CA, Simonneau M, O'Donnell JM, MacDermott AB, Karayiorgou M, Gogos JA (2011) Altered axonal targeting and short-term plasticity in the hippocampus of Disc1 mutant mice. Proc Natl Acad Sci USA 108:E1349–E1358

Le Strat Y, Ramoz N, Gorwood P (2009) The role of genes involved in neuroplasticity and neurogenesis in the observation of a gene-environment interaction (G×E) in schizophrenia. Curr Mol Med 9:506–518

Li W, Zhou Y, Jentsch JD, Brown RA, Tian X, Ehninger D, Hennah W, Peltonen L, Lonnqvist J, Huttunen MO, Kaprio J, Trachtenberg JT, Silva AJ, Cannon TD (2007) Specific developmental disruption of disrupted-in-schizophrenia-1 function results in schizophrenia-related phenotypes in mice. Proc Natl Acad Sci USA 104:18280–18285

Li B, Chen F, Ye J, Chen X, Yan J, Li Y, Xiong Y, Zhou Z, Xia J, Hu Z (2010) The modulation of orexin A on HCN currents of pyramidal neurons in mouse prelimbic cortex. Cereb Cortex 20:1756–1767

Liao CC, Lee LJ (2011) Neonatal fluoxetine exposure affects the action potential properties and dendritic development in cortical subplate neurons of rats. Toxicol Lett 207:314–321

Liao CC, Lee LJ (2012) Evidence for structural and functional changes of subplate neurons in developing rat barrel cortex. Brain Struct Funct 217:275–292

Mackie S, Millar JK, Porteous DJ (2007) Role of DISC1 in neural development and schizophrenia. Curr Opin Neurobiol 17:95–102

Manoach DS (2003) Prefrontal cortex dysfunction during working memory performance in schizophrenia: reconciling discrepant findings. Schizophr Res 60:285–298

Mao Y, Ge X, Frank CL, Madison JM, Koehler AN, Doud MK, Tassa C, Berry EM, Soda T, Singh KK, Biechele T, Petryshen TL, Moon RT, Haggarty SJ, Tsai LH (2009) Disrupted in schizophrenia 1 regulates neuronal progenitor proliferation via modulation of GSK3beta/beta-catenin signaling. Cell 136:1017–1031

Mei L, Xiong WC (2008) Neuregulin 1 in neural development, synaptic plasticity and schizophrenia. Nat Rev Neurosci 9:437–452

Meyer-Lindenberg A (2010) From maps to mechanisms through neuroimaging of schizophrenia. Nature 468:194–202

Millar JK, Wilson-Annan JC, Anderson S, Christie S, Taylor MS, Semple CA, Devon RS, St Clair DM, Muir WJ, Blackwood DH, Porteous DJ (2000) Disruption of two novel genes by a translocation co-segregating with schizophrenia. Hum Mol Genet 9:1415–1423

Millar JK, Pickard BS, Mackie S, James R, Christie S, Buchanan SR, Malloy MP, Chubb JE, Huston E, Baillie GS, Thomson PA, Hill EV, Brandon NJ, Rain JC, Camargo LM, Whiting PJ, Houslay MD, Blackwood DH, Muir WJ, Porteous DJ (2005) DISC1 and PDE4B are interacting genetic factors in schizophrenia that regulate cAMP signaling. Science 310:1187–1191

Moghaddam B, Homayoun H (2008) Divergent plasticity of prefrontal cortex networks. Neuropsychopharmacology 33: 42–55

Nataraj K, Le Roux N, Nahmani M, Lefort S, Turrigiano G (2010) Visual deprivation suppresses L5 pyramidal neuron excitability by preventing the induction of intrinsic plasticity. Neuron 68:750–762

Niwa M, Kamiya A, Murai R, Kubo K, Gruber AJ, Tomita K, Lu L, Tomisato S, Jaaro-Peled H, Seshadri S, Hiyama H, Huang B, Kohda K, Noda Y, O'Donnell P, Nakajima K, Sawa A, Nabeshima T (2010) Knockdown of DISC1 by in utero gene transfer disturbs postnatal dopaminergic maturation in the frontal cortex and leads to adult behavioral deficits. Neuron 65:480–489

Penzes P, Cahill ME, Jones KA, VanLeeuwen JE, Woolfrey KM (2011) Dendritic spine pathology in neuropsychiatric disorders. Nat Neurosci 14:285–293

Pletnikov MV, Ayhan Y, Nikolskaia O, Xu Y, Ovanesov MV, Huang H, Mori S, Moran TH, Ross CA (2008) Inducible expression of mutant human DISC1 in mice is associated with brain and behavioral abnormalities reminiscent of schizophrenia. Mol Psychiatry 13:173–186

Robinson RB, Siegelbaum SA (2003) Hyperpolarization-activated cation currents: from molecules to physiological function. Annu Rev Physiol 65:453–480

Santini E, Porter JT (2010) M-type potassium channels modulate the intrinsic excitability of infralimbic neurons and regulate fear expression and extinction. J Neurosci 30:12379–12386

Schurov IL, Handford EJ, Brandon NJ, Whiting PJ (2004) Expression of disrupted in schizophrenia 1 (DISC1) protein in the adult and developing mouse brain indicates its role in neurodevelopment. Mol Psychiatry 9:1100–1110

Shen S, Lang B, Nakamoto C, Zhang F, Pu J, Kuan SL, Chatzi C, He S, Mackie I, Brandon NJ, Marquis KL, Day M, Hurko O, McCaig CD, Riedel G, St Clair D (2008) Schizophrenia-related neural and behavioral phenotypes in transgenic mice expressing truncated Disc1. J Neurosci 28:10893–10904

Spruston N (2008) Pyramidal neurons: dendritic structure and synaptic integration. Nat Rev Neurosci 9:206–221

Steinecke A, Gampe C, Valkova C, Kaether C, Bolz J (2012) Disrupted-in-Schizophrenia 1 (DISC1) is necessary for the correct migration of cortical interneurons. J Neurosci 32:738–745

Tan HY, Callicott JH, Weinberger DR (2007) Dysfunctional and compensatory prefrontal cortical systems, genes and the pathogenesis of schizophrenia. Cereb Cortex 17(Suppl 1):i171–i181

Volk DW, Lewis DA (2010) Prefrontal cortical circuits in schizophrenia. Curr Top Behav Neurosci 4:485–508

Wang Q, Charych EI, Pulito VL, Lee JB, Graziane NM, Crozier RA, Revilla-Sanchez R, Kelly MP, Dunlop AJ, Murdoch H, Taylor N, Xie Y, Pausch M, Hayashi-Takagi A, Ishizuka K, Seshadri S, Bates B, Kariya K, Sawa A, Weinberg RJ, Moss SJ, Houslay MD, Yan Z, Brandon NJ (2011) The psychiatric disease risk factors DISC1 and TNIK interact to regulate synapse composition and function. Mol Psychiatry 16:1006–1023

Zhou X, Geyer MA, Kelsoe JR (2008) Does disrupted-in-schizophrenia (DISC1) generate fusion transcripts? Mol Psychiatry 13:361–363

Zhou X, Chen Q, Schaukowitch K, Kelsoe JR, Geyer MA (2010) Insoluble DISC1-Boymaw fusion proteins generated by DISC1 translocation. Mol Psychiatry 15:669–672

Zucker RS, Regehr WG (2002) Short-term synaptic plasticity. Annu Rev Physiol 64:355–405